Turbulent magnetohydrodynamic natural convection in a heat pipe assisted cavity using disk-shaped magnesium ferrite nanoparticles

K. Ajith[1], Mallolu Jesse Aaron[1], Archana Sumohan Pillai[2], I.V. Muthuvijayan Enoch[2], A. Brusly Solomon[1, *], M. Sharifpur[3,4*], J.P. Meyer[3]

[1]Micro and Nano Heat Transfer Lab, Centre for Research in Material Science and Thermal Management, Department of Mechanical Engineering, Karunya Institute of Technology and Sciences, Coimbatore, India

[2]Department of Chemistry & Department of NanoScience, Karunya Institute of Technology and Sciences, Coimbatore, India

[3]Department of Mechanical and Aeronautical Engineering, University of Pretoria, Pretoria 0002, South Africa

[4]Department of Medical Research, China Medical University Hospital, China Medical University, Taichung, Taiwan

Corresponding Author: * abruslysolomon@gmail.com
**Mohsen.Sharifpur@up.ac.za

Abstract

The prospect to alter the thermophysical properties of ferrofluid with an influence of magnetic field leads to improving natural convection in various heat transfer systems. This investigation principally focuses on the studies of electromagnetism-based turbulent natural convection heat transfer of low-density disk-shaped magnesium ferrite /water-based ferrofluid, filled in a novel heat pipe-assisted cubical cavity at various volume fractions. Two flat plate heat pipes were used to maintain temperature differences in the cavity. To advance the buoyancy of working fluid inside the cavity, deliberately low-density ferrofluid containing disk-shaped particles were formulated using the hydrothermal method. The temperature difference between the two-heat pipe-assisted vertical walls were sustained with four distinct temperature ranges from 10 to 25 ºC. The ferrofluid filled in the cavity was then subjected to magnetic field ranging from 0 to 350 Gauss to understand the thermomagnetic convection effects on heat transfer. The optimal volume fraction of ferrofluid for maximum heat transfer was found to be 0.05% at a wall temperature difference of 25 ºC, owing to 23.51% improvement in average heat transfer coefficient along with 33.37% improvement in average Nusselt number when compared to water. With the application of a magnetic field of 350 Gauss, the average heat transfer coefficient was further enhanced by 10.11%, and the average Nusselt number improved by 6.28% for 0.05% volume fraction in comparison to the condition where no magnetic field was applied.

Keywords: Natural convection; Heat pipe; Ferrofluid; Magnetic field; Magnesium ferrite; Turbulent flow

Introduction

Utilization of renewable energy sources has the potential to save the environment from the consequences of global warming, energy scarcity, and climate change caused by the overconsumption of fossil fuels to meet our energy requirements. Therefore, it is absolutely necessary to use renewable energy and to improve the operational efficiency of renewable energy systems. The solar PV system is one of the most commonly used systems for generating electricity from incident sunlight with the aid of solar cells. However, only a small quantity of incident light is transformed into electricity, and most of the light energy is converted into heat by the solar PV-panel surfaces. The temperature of the panel surface will rise due to absorbed solar radiation and lower the performance of solar PV systems (Ahmed et al. 2019). Therefore, to improve the efficiency of solar PV systems, it is mandatory to remove the excess heat generated in the solar PV panel surface. In the past, conventional cooling fluids such as thermal oil, water, refrigerant, and ethylene glycol were used for reducing the PV-panel surface temperature (Elsheikh et al. 2018; Sathyamurthy et al. 2021). However, the thermo-physical properties of conventional cooling fluids are known to be insubstantial to make them effective for use in cooling PV-panel surfaces.

Nanofluid (NF) is a colloidal mixture of nanomaterials and conventional cooling fluids formulated to boost the heat transfer properties of conventional cooling fluids (Choi 1995). Additionally, NFs have many different applications in energy/catalysis research (Ghasemi et al. 2020, 2021; Mozaffari et al. 2021). There are wide range of investigations carried out for improving the thermo-physical properties of conventional fluids by suspending different types of nanoparticles of various sizes (less than 100 nm) into them. It was concluded that the thermophysical properties of the NF was enhanced with a rise in nanoparticles quantity in base fluids (Gaganpreet and Srivastava 2012; Nkurikiyimfura et al. 2013; Solangi et al. 2015; Shah et al. 2017; Sezer et al. 2019). Further, the addition of hybrid nanoparticles into the conventional fluid was found to be one of the effective methods for improving the thermo-physical properties of conventional fluids (Soltani and Akbari 2016; Akilu et al. 2017). Apart from NF and hybrid NF, Ferrofluids (FFs) were formulated by dispersing magnetic nanoparticles into the traditional cooling fluids for enhancing its thermo-physical properties by applying an external magnetic field (MF). From the reviews (Kumar and Subudhi 2017; Doganay et al. 2019), it was evident that the application of MF on the FF can enhance the thermal conductivity and viscosity of FF significantly. To study the effectiveness of NFs in various thermal systems, natural convection heat transfers in cavities filled with different NFs were investigated and it was concluded that the heat transfer capacity of NFs was enhanced at lower volume concentrations. However, the heat transfer capacity of NFs was reduced due to its high viscosity and density at higher concentrations (Hu et al. 2014; Choudhary and Subudhi 2016; Ghodsinezhad et al. 2016; Garbadeen et al. 2017; Solomon et al. 2017). Giwa et al.(2019) experimentally investigated the use of hybrid NF (Al_2O_3: MWCNT/H_2O) in the square cavity for the free convection heat transfer. The hybrid NF was prepared at various weight percentages of Al_2O_3 / MWCNT nanoparticles and the results revealed that the water-based NF with 60:40 weight percentage of Al_2O_3: MWCNT enhanced the natural convection heat transfer in terms of Nusselt number by 16.2% and average heat transfer coefficient by 20.5% compared to that of water.

Besides this, a new way of enhancing the natural convection heat transfer with FF in the enclosure through regulating fluid movement by means of MF was proposed in few studies (Sheikholeslami and Rokni 2017; Giwa et al. 2020a). Some studies show the importance of using sensitivity analysis and artificial intelligence to obtain more precise predictions (Ebrahimi et al. 2021; Wang et al. 2021). Very few experimental investigations were also conducted to examine the impact of MF on the natural convection heat transfer by using FFs filled clear enclosure (Giwa et al. 2021; Narankhishig et al. 2021). Joubert et al.(2017) studied the laminar natural convection heat transfer augmentation using Fe_3O_4/H_2O FF of different concentrations in a square enclosure subjected to MF. It was shown that the optimum heat-transfer performance was attained at a volume fraction of 0.10% by improving the Nu_{avg} by 5.63%. In the presence of MF, the Nu_{avg} again enhanced to 2.81%. Shi et al.(2019) analyzed the laminar natural convection heat transfer by utilizing hybrid NF consisting of Fe_3O_4: CNT (2:1)/Water FF with the MF application in the rectangular cavity. The heat transfer was enhanced maximum by 15% without the application of the MF. Later the application of MF (400 Gauss) enhanced the heat transfer from15% to 24%. Dixit and Pattamatta (2019) studied the influence of MF strength (0.13 to 0.3 Tesla) and MF direction on laminar natural convection heat transfer of four different NFs (multi-wall carbon nanotubes NF, graphene NF, copper NF, and silica NF) filled in a cubical cavity whose vertical sides were kept at different temperatures. The results concluded that the natural convection heat transfer capacity of MWCNT /water NF (0.10% volume fraction) and Graphene NF (0.057% volume fraction) were enhanced by 12% and 13% respectively without the application of MF. Also, there was no improvement in the heat transfer performance of copper NF and silica NF compared to that of water under the condition stated above. Moreover, the heat transfer performance of all NFs reduced over water when the MF was applied in the range between 0.13 to 0.3 Tesla. Dixit and Pattamatta (2020) analyzed the laminar natural convection heat transfer in a differentially heated cubical cavity, employing two different FFs such as Fe_3O_4/H_2O and Fe/H_2O at volume fractions of 0.05% and 0.20% with the application of MF strength of 0.3 Tesla. It was understood that the direction of the MF lines has an important role in the enhancement of natural convection heat transfer. It was concluded that the influence of direction of the MF reduced the transfer of heat for both FFs and this reduction was proportional to the volume fraction. Giwa et al. (2020b) identified the finest volume percentage for maximum heat transfer enhancement (10.79%) as 0.10% of Ferrite: Alumina/ H_2O hybrid FFs in a rectangular enclosure whose sidewalls are maintained at a temperature difference of 35 ^oC. Further, it was noted that the natural convection heat transfer was improved again by 4.91% at MF strength of 118.4 Gauss in the tested range of 48.9 to 219.5 Gauss.

Besides the heat transfer enhancement reported above, various boundary conditions imposed on the cavities were summarised in Table 1. It was noted that equipment's like shell and tube heat exchangers, thermostatic water baths, and tape heaters are commonly used to establish heating and cooling boundary conditions and these conditions can be non-uniform. Moreover, the use of conventional heat exchangers and thermostatic water baths requires external power for operation and it makes the system more complex. Hence, a flat heat pipe heat spreader is used to maintain uniform temperature at the hot and cold sidewall of the cavity. It was also observed from the table that there are different magnetic nanoparticles with different morphology such as spherical, flakes, bricks, and hybrid of spherical, and tubular structures and these shapes have lower aspect ratio than disk shape nanoparticles. Literature confirms that the nanoparticles having a high aspect ratio provides better thermal conductivity and better viscosity for NFs. In this study, the type of nanoparticle is selected based on the density of particle expecting that a low-density nanofluid is required to increase buoyancy and thereby improve the natural convection process. A prior experimental study by Ajith et al. (2020)

Table 1 Observations from investigations employed ferrofluids in the cavity with MF application

Authors	Nanofluid	Nanoparticle shape	Geometry of the cavity	Heating and cooling methods	Magnetic field (Gauss)	Natural convection heat transfer enhancement
Joubert et al.(2017)	Fe_2O_3+ Water	Fe_2O_3- Spherical	Square	Copper shell and tube heat exchanger at both sides	300 and 700 Gs	5.63% enhancement in Nu at volume fraction of 0.10% over base fluid. Additional increase of 2.81% at MF 700 Gauss for the same volume fraction
Shi et al..(2019)	Fe_3O_4: CNT + Water	Fe_3O_4-Spherical CNT-Tubular	Rectangular	Silica gel heater with DC supply at hot side and thermostatic water bath	50 to 400 Gs	15% enhancement in Natural convection heat transfer at 2:1 mass fraction. Heat transfer efficiency enhanced from 15% to 24% with the application of MF of 400 Gauss
Dixit and Pattamatta (2020)	Fe_3O_4 + Water and Fe + Water	Fe_3O_4- Brick shape Fe-Brick shape	Cubical	Nichrome wire heater with DC supply at hot side and cold plate with cold bath	3000 Gs	The influence of MF direction reduced the heat transfer rate of both NFs
Dixit and Pattamatta (2019)	MWCNT nanofluid, Graphene nanofluid, copper nanofluid, and silica nanofluid	MWCNT- Tubular Graphene-Flat flake Copper-Spherical Silica-Spherical	Cubical	Nichrome wire heater with DC supply at hot side and cold plate with cold bath	1300 and 3000 Gs	Heat transfer performance of MWCNT /water NF at 0.10% VF and Graphene NF at 0.057 VF were enhanced by 12% and 13% respectively. Heat transfer performance of all NF diminished by the influence of MF
Giwa et al.(2020b)	Fe_2O_3:Al_2O_3 + Water	Fe_2O_3-Spherical Al_2O_3-Spherical	Rectangular	Counter flow shell and tube heat exchanger at both sides	48.9 to 219.5 Gs	10.81% enhancement in Nu number at 0.10vol% FF and additional enhancement of 4.91% at MF of 219Gauss.
Giwa et al.(2020c)	Fe_2O_3: MWCNT + Water	Fe_2O_3- Spherical MWCNT-Tubular	Rectangular	Counter flow shell and tube heat exchanger at both sides	48.9 to 219.5 Gs	Heat transfer performance enhanced maximum by 11.21% for 0.05% volume fraction and additional 5.02% enhancement at MF 219.5 Gauss

authenticates that $MgFe_2O_4$/Water-based FF with disk shape has considerable enhancement in thermal conductivity with MF application compared to water. Further, it was reported that the density of $MgFe_2O_4$ FF was low compared to other FFs and was reduced by the influence of MF. It was pointed out that the rise in the viscosity of $MgFe_2O_4$ FF by the influence of MF was low related to that of other FFs(Doganay et al. 2019; Ajith et al. 2021). These features of $MgFe_2O_4$ FF led to the analysis of its feasibility in magnetohydrodynamic natural convection heat transfer. Moreover, limited experimental studies on magnetohydrodynamic laminar natural convection were available (Kumar and Subudhi 2017; Giwa et al. 2020a, 2021) and no work has been published on the magnetohydrodynamic turbulent natural convection heat transfer in the cavity using FF with disk shape nanoparticles. Therefore, this study is focused on the experimental analysis of magnetohydrodynamic turbulent natural convection heat transfer in the heat pipe-assisted cubical cavity with aid of high aspect ratio disk-shaped $MgFe_2O_4$ nanoparticles in base fluids.

Methodology

Ferrofluid formulation

Magnesium ferrite ($MgFe_2O_4$) nanoparticle was synthesized by hydrothermal method using mixtures of ferric and magnesium nitrate solutions (Ajith et al. 2019, 2020). The dimension and structure of the prepared $MgFe_2O_4$ nanoparticles are examined by the SEM and TEM analysis as represented in Figure 1(a) and (b). The $MgFe_2O_4$ nanoparticles synthesized are in disk shape with a diameter of ≈93 nm. To make the FF, $MgFe_2O_4$ nanoparticles were dispersed in water. For the better homogenization of FF, a Hielscher UP400S ultrasonic mixer was utilized for 40 minutes and prepared 1 litre of solution. After the sonication process, sodium dodecyl sulfate (SDS) was added to the fluid and sonicated for 20 minutes for improving stability. The mass of SDS added to the fluid is the same as the mass of nanoparticles added to water for the preparation of FF (Joubert et al. 2017). Yu et al. 2010 studied the long-term stability of the NF by measuring its thermal conductivity for a certain experimental time of 360 minutes. Hence, To check the long term stability of $MgFe_2O_4$ FF in our study, the thermal conductivity of FF at various volume fractions (0.01,0.05, and 0.10 %) is measured over a 15-week duration at a temperature of 25^{o}C and it is revealed that the FF is stable over a 15-week duration with a constant thermal conductivity as depicted in Figure 2. This result confirms the prepared FF is possessed long-term stability.

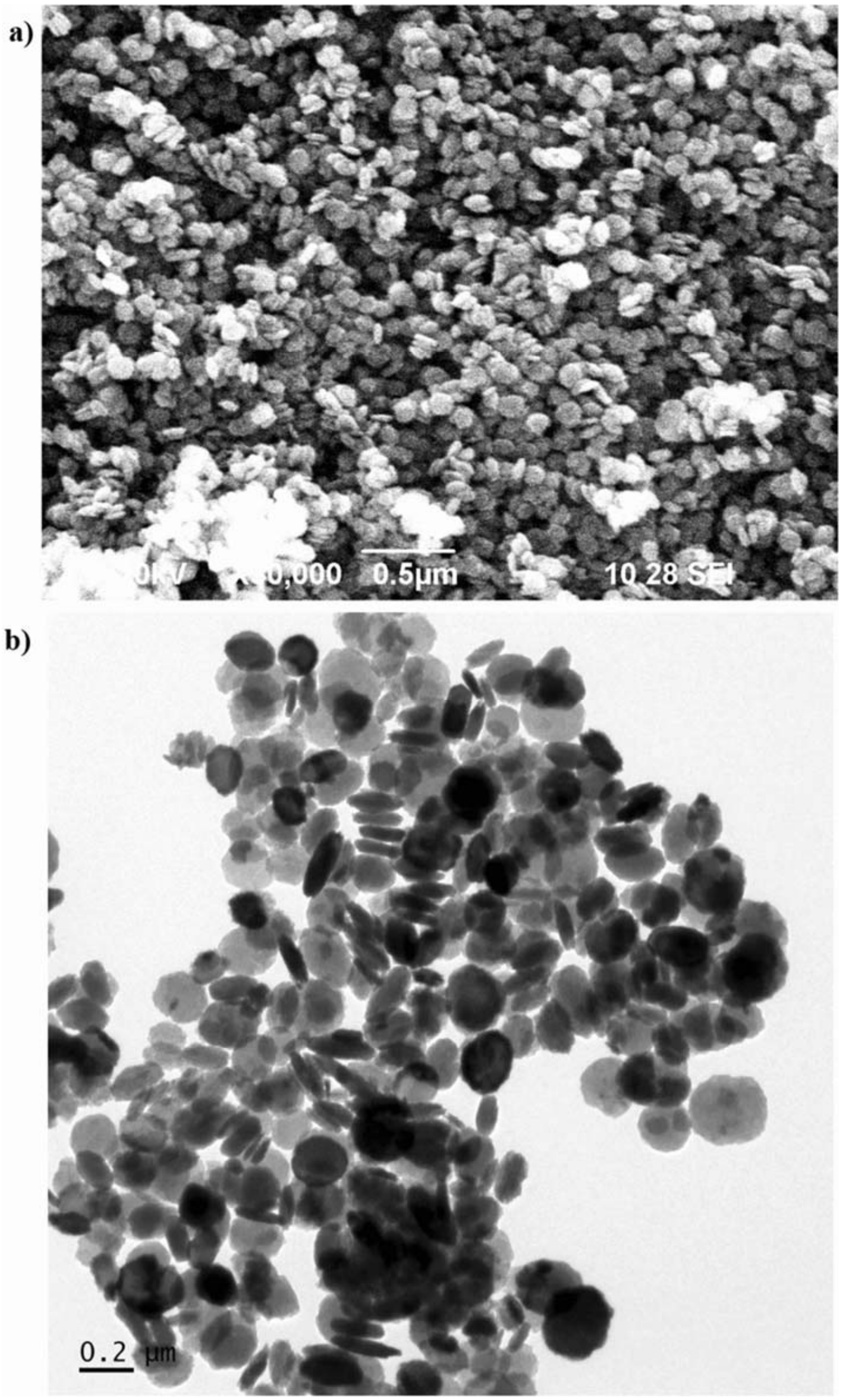

Fig. 1 Microscopic view of $MgFe_2O4$ magnetic nanoparticles a) SEM image; b) TEM image

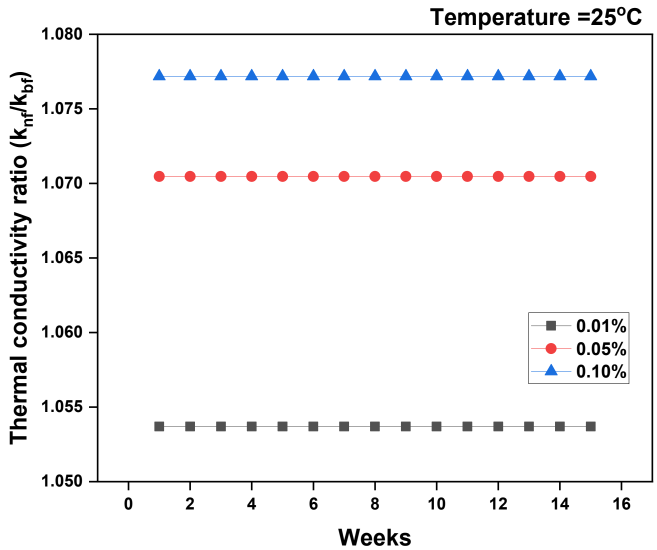

Fig. 2 Stability of prepared Ferrofluid through its thermal conductivity

Experimental setup

The layout of the experimental testing facility for the magnetohydrodynamic natural convection study is shown in Figure 3. The experimental testing facility comprises of heat pipe-assisted cubical cavity with dimensions L (100) × W (100) × H (100) mm, heater, water pump, chiller, data logger, computer, dimmer stat, electromagnets, and DC power supply. The two vertical sides of the cavity are covered with two flat heat pipes and all other sides including the bottom were covered with an acrylic sheet of thickness 10 mm. The application of heat pipe provides a uniform temperature on both sides of the cavity to predict the heat transfer capability accurately. A heat pipe is a passive heat transfer device that utilizes the principles of both boiling and condensation to transfer heat from one position to another. Generally, the heat pipe consists of a metal enclosure, working fluid, and a wick structure to transport the liquid. The working fluid undergoes a phase change (evaporation to condensation and vice versa) to transfer the heat depending on the temperature. The wick material in the heat pipe returns the condensate liquid to the evaporator through capillary action. The heat pipe can maintain a consistent temperature at the cavity's heat transfer surface, increasing precision and serving as the cavity's heating and cooling boundary state. The use of conventional heat exchangers requires external power for its working and it makes the system more complex. Hence in this study, for the heating and cooling of FFs, two flat heat pipes were fabricated and fixed on the two sides of the cavity at a distance of 100 mm and this cubical cavity is covered with glass wool housed in a wooden box. The cold side heat pipe is cooled using a constant temperature bath and the hot side heat pipe is attached with a heater. A dimmer stat is used to control the power supply to the heater, the power input is changed by varying the voltage.

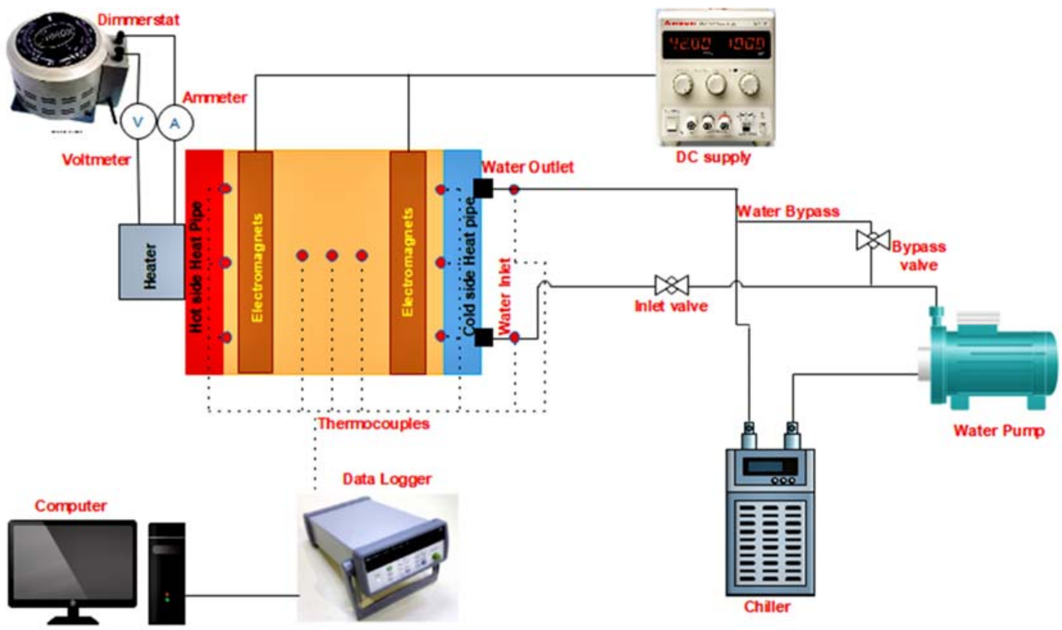

Fig. 3 Layout of Experimental setup for natural convection heat transfer

There are five T-type thermocouples each welded on both the hot side and cold side heat pipe of the inner cavity for wall surface temperature measurement. Another five T-type thermocouples are attached along the canter of the cavity for FF temperature measurement. Two thermocouples are fixed to measure the inlet and outlet temperature of cooling water supplied to the condenser of the cold side heat pipe. The arrangement of the thermocouples in the experimental setup is displayed in Figure 4 and all these thermocouples are connected to the HP Agilent Key sight data logger (34972A), which records all temperature readings. Four electromagnets (which contain a core of 10 cm length and number of copper windings of 1200) delivered the MF once it is linked to the DC power supply. Two of these electromagnets are kept on the upper portion and two at the lower portion of the cavity as shown in Figures 5 (a) and (b). The magnets are placed in such a way that the direction of MF lines is perpendicular to the direction of heat transfer from the hot side to the cold sidewall as presented in Figure 5(c). A Gauss meter was used to measure the MF strength provided by the electromagnets. A water pump is installed to supply cold water into the cold side heat pipe and to extract the heat. The cold-water temperature is maintained by a chiller. A rotameter is connected to the pump to monitor and to maintain the inlet water flow rate.

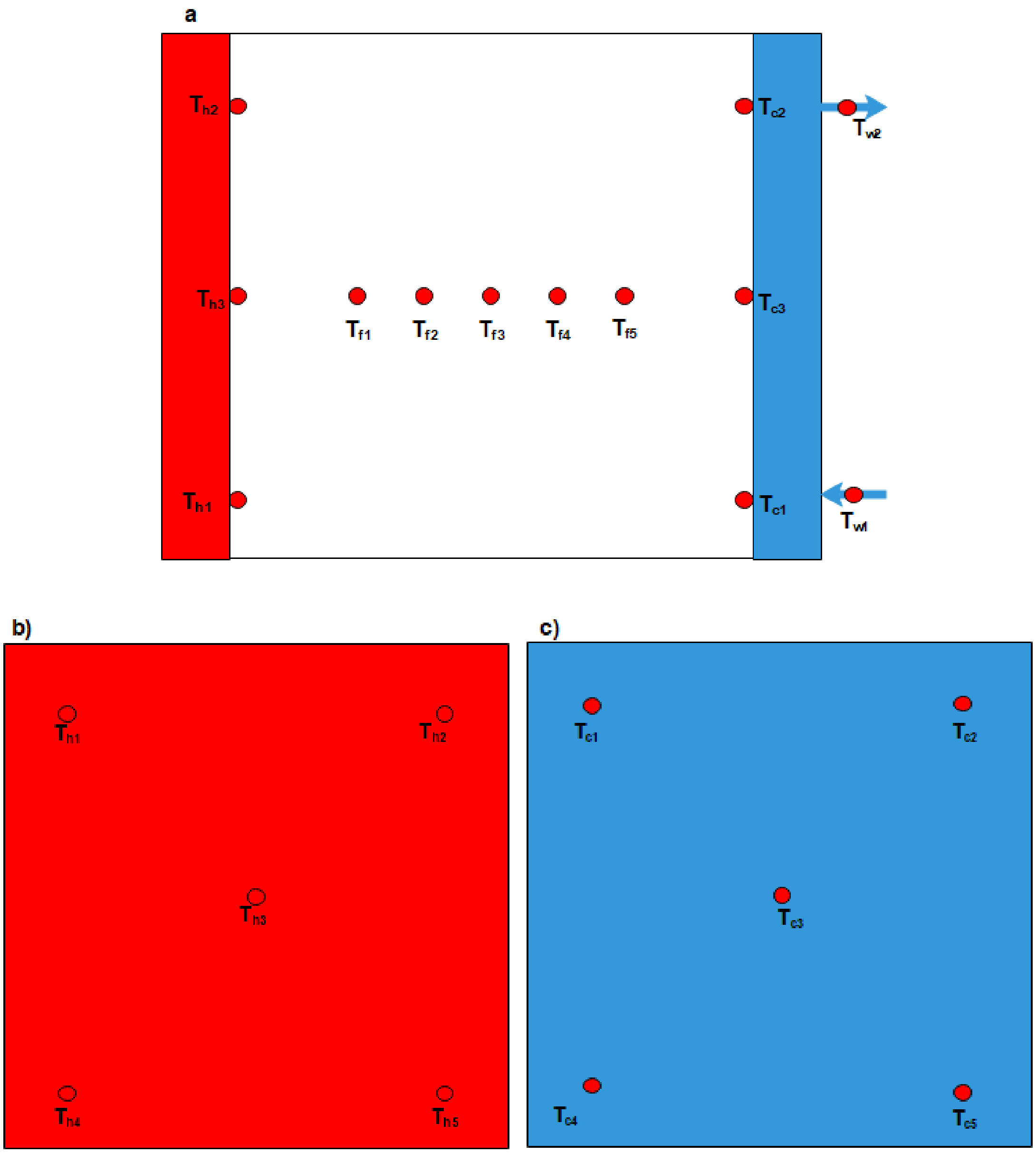

Fig. 4 Thermocouple position a) Within the cavity; b) Within the hot sidewall; and c) Within the cold sidewall of the cavity

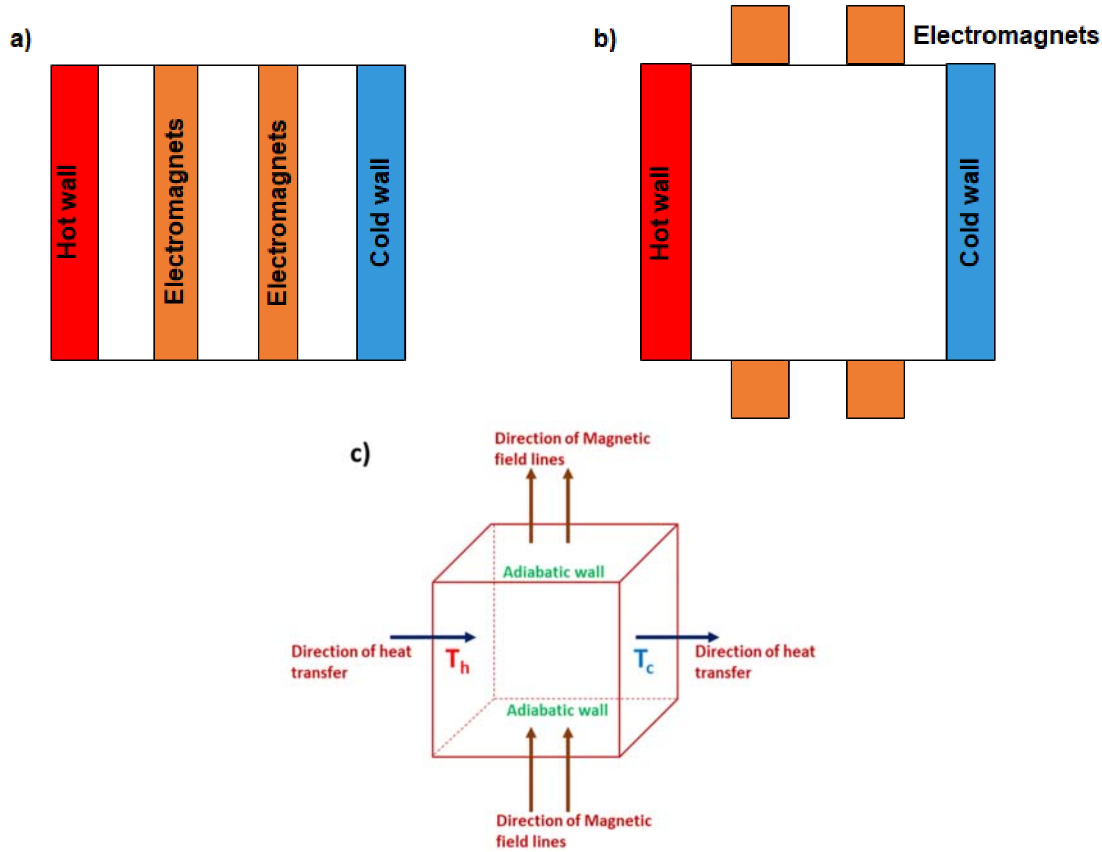

Fig. 5 Position of electromagnets on the cubical cavity a) Top view; b) Side view; and c) Direction of magnetic field lines

Experimental procedure

The cubical cavity is filled with 1000 ml of $MgFe_2O_4$ FF at various volume fractions. The ΔT_{hc} is kept at 10, 15, 20, and 25 °C by setting the power input at the hot side heat pipe and maintaining the low temperature on the other side of the cavity by supplying cooling water to the cold side of the heat pipe. At different ΔT_{hc}, the temperature of the hot sidewall, working fluid, and cold side wall was noted for about 40 minutes till the experimental system attains a steady-state condition. Then, electromagnets were powered to apply 50 Gauss of MF about 30 minutes to attain a steady-state, and this process was continued till 350 Gauss. At each 50 Gauss MF application, the temperature responses were recorded. The sidewalls and bottom of the cavity are inspected in every experiment and no noticeable nanoparticles deposition observed. This ensures that the prepared nanofluid is stable under the magnetic field for the entire experimental duration. Besides, the stability of $MgFe_2O_4$ FF filled in the cavity may degrade at elevated temperatures and the nanoparticles may deposit at the heat exchanging surfaces.

Therefore, to avoid the stability issues the ΔT_{hc} between the hot and cold side of the cavity is maintained at a lower temperature difference ranging from 10 to 25°C.

Solution methodology

The heat transfer capacity of the cubical cavity was analyzed by heat balance test after determining the heat input to the cavity (Q_{in}) and heat output from the cavity (Q_{out}). Also, the hot side heat transfer coefficient (h_{hot}), cold side heat transfer coefficient (h_{cold}), average heat transfer coefficient of the cavity (h_{avg}), and average Nusselt number (Nu_{avg}) for varying Rayleigh number (Ra) are estimated to analyze the heat transfer in the cavity.

Heat supplied to the FF (Q_{in}) is estimated using power supplied to heater attached to the hot side heat pipe using the Eq. (1)

$$Q_{in} = V * I \quad (1)$$

Heat transferred by the cavity (Q_{out}) from the cold side heat pipe is determined by Newton's law of cooling as presented in Eq. (2)

$$Q_{out} = m_w * C_{p(w)} * \Delta T_w \quad (2)$$

Heat transfer coefficients h_{hot} and h_{cold} are measured using Eq. (3) and (4)

$$h_{hot} = \frac{Q_{in}}{A(T_h - T_f)} \quad (3)$$

$$h_{cold} = \frac{Q_{out}}{A(T_f - T_c)} \quad (4)$$

Based on the h_{hot} and h_{cold}, the average heat transfer coefficient was calculated as shown in Eq. (5)

$$h_{avg} = \frac{h_{hot} + h_{cold}}{2} \quad (5)$$

The average Nusselt number Nu_{avg} of the cavity is calculated as

$$Nu_{avg} = \frac{h_{avg} * L_c}{k_{wf}} \quad (6)$$

The nature of flow inside the cavity is determined by calculating the Ra and is expressed as in Eq. (7)

$$Ra = \frac{g\beta_{wf}[T_h - T_c]\rho_{wf}{}^2 (C_{pwf})(L_c{}^3)}{(\mu_{wf})(k_{wf})} \quad (7)$$

The specific heat of the FF is estimated by using the correlation as shown in Eq. (8)

$$\rho_{nf} C_{p_{nf}} = \phi_{nf} \rho_{np} c_{p_{np}} + (1-\phi_{nf}) \rho_{bf} C_{p_{bf}} \quad (8)$$

Based on the Prandtl number and Ra number, the Berkovsky and Polevikov model expressed in Eq. (9) is used to validate the experimental data (B. Berkovsky). In this study, the Prandtl number is less than 10^5 and the Ra is less than 10^{10}.

$$Nu = 0.18[\left(\frac{Pr}{0.2+Pr}\right)(Ra)]^{0.29} \quad (9)$$

In this study, the thermal conductivity, viscosity, and density of $MgFe_2O_4$ FF in the absence and presence of MF were taken from the thermo-physical properties of $MgFe_2O_4$ FF reported by Ajith et al. (2020) as presented in Table 2.

Table 1 Thermophysical properties of $MgFe_2O_4$ ferrofluid at various volume fractions subjected to magnetic field

Temperature (°C)	Magnetic field (Gauss)	Thermo-physical properties								
		k (W/mK)			μ (Cp)			ρ (kg/m³)		
		0.01%	0.05%	0.10%	0.01%	0.05%	0.10%	0.01%	0.05%	0.10%
25	0	0.628	0.639	0.642	0.921	0.994	1.055	1003.417	1014.19	1027.941
25	100	0.632	0.644	0.646	0.933	1.002	1.064	1001.813	1012.814	1025.649
25	200	0.638	0.649	0.653	0.945	1.012	1.074	999.7503	1010.752	1023.128
25	250	0.640	0.652	0.657	0.950	1.017	1.078	998.8336	1009.606	1021.753
25	300	0.643	0.656	0.660	0.956	1.023	1.08	997.9168	1008.46	1019.92
25	350	0.645	0.661	0.664	0.961	1.027	1.084	988.5505	1000.183	1011.816

Uncertainty analysis

The uncertainty in the experimental measurement of Q_{in}, Q_{out}, h_{hot}, h_{cold}, and Nu_{avg} were calculated by using Eqs. (10) to (14) and the same are presented in Table 3.

$$\delta Q_{in} = \sqrt{\left(\frac{\Delta V_{in}}{V_{in}}\right)^2 + \left(\frac{\Delta I_{in}}{I_{in}}\right)^2} \quad (10)$$

$$\delta Q_{out} = \sqrt{\left(\frac{\partial Q_{out}}{\partial m_w}\delta m_w\right)^2 + \left(\frac{\partial Q_{out}}{\partial C_{pw}}\delta C_{p_w}\right)^2 + \left(\frac{\partial Q_{out}}{\partial \Delta T_w}\delta \Delta T_w\right)^2} \quad (11)$$

$$\delta h_{hot} = \sqrt{\left(\frac{\partial h_h}{\partial Q_{in}}\delta Q_{in}\right)^2 + \left(\frac{\partial h_h}{\partial A}\delta A\right)^2 + \left(\frac{\partial h_h}{\partial T_h}\delta T_{hot}\right)^2 + \left(\frac{\partial h_h}{\partial T_f}\delta T_{fluid}\right)^2} \quad (12)$$

$$\delta h_{cold} = \sqrt{\left(\frac{\partial h_c}{\partial Q_{out}}\delta Q_{out}\right)^2 + \left(\frac{\partial h_c}{\partial A}\delta A\right)^2 + \left(\frac{\partial c}{\partial T_f}\delta T_{fluid}\right)^2 + \left(\frac{\partial h_c}{\partial T_c}\delta T_{cold}\right)^2} \quad (13)$$

$$\delta Nu = \sqrt{\left(\frac{\partial Nu}{\partial h}\delta h_{avg}\right)^2 + \left(\frac{\partial Nu}{\partial L}\delta L\right)^2 + \left(\frac{\partial Nu}{\partial k_{nf}}\delta k_{nf}\right)^2} \quad (14)$$

Table 2 Uncertainty in various estimations

Parameters	Average Uncertainty
Heat input (Q_{in})	3.35%
Heat output (Q_{out})	8.20%
Heat transfer coefficient at hot sidewall (h_h)	5.07%
Heat transfer coefficient at cold sidewall(h_c)	9.15%
Nusselt number (Nu)	5.76%

Results and Discussion

Validation of the Results

The experimental Nu_{avg} is validated against the theoretical Nu_{avg} determined using Berkovsky and Polevikov model as shown in Eq. 9 and the results are presented in Figure 6. It is found that the experimental and theoretical Nu_{avg} are linearly increasing with increasing Ra and following an identical trend.

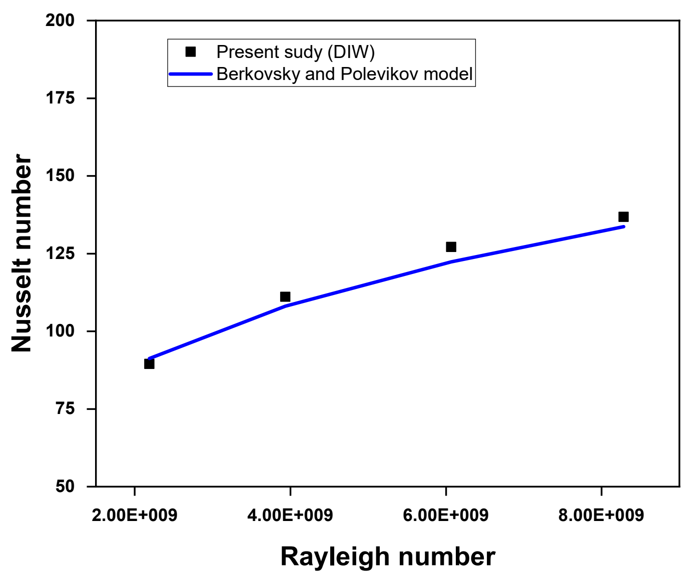

Fig. 6 Validation of the results with Berkovsky and Polevikov model (B. Berkovsky).

Hot side heat transfer coefficient of the cavity

The effect of the changing volume fraction of $MgFe_2O_4$ FF on the h_{hot} at different ΔT_{hc} is calculated using Eq.3 and shown in Figure 7(a). By using the $MgFe_2O_4$ FF as a working fluid, h_{hot} of the cavity is enhanced in relation to that of water and it improved with the rise of ΔT_{hc} from 10 to 25 ºC. The h_{hot} of the cavity at volume fraction 0.01%, 0.05%, and 0.10% is greater than that of the water, and maximum enhancement of 48.13% was observed at ΔT_{hc} = 25 ºC with 0.05% volume fraction. Though the h_{hot} is increased till the FF volume percent of 0.05, the same is inferior to 6% when the volume fraction is increased to 0.10%. It is known that the h_{hot} of the cavity depends on factors such as hot sidewall temperature, working fluid temperature, and the thermophysical properties of the working fluid. If the working fluid possesses high thermal conductivity, more amount of heat will be transferred from the hot sidewall to the working fluid. By increasing the ΔT_{hc} from 10 to 25 ºC, the temperature of the hot sidewall increases from 22 to 55 ºC. Due to this higher temperature of the hot sidewall, the Brownian motion of nanoparticles is higher, consequently, its thermal conductivity increases compared to water. Further, the thickness of the thermal boundary layer also reduces due to the enhanced Brownian motion of nanoparticles, which augments the transfer of heat from the hot sidewall to $MgFe_2O_4$ FF, thus enhancing the h_{hot} (Mojumder et al. 2015; Vanaki et al. 2016; Sha et al. 2017). Simultaneously, the viscosity and density of the FF near the hot sidewall reduces. Subsequently, FF adjacent to the hot sidewall becomes low dense and gradually goes up along the hot sidewall, and this low dense fluid travels to the cold side region of the cavity in a clockwise direction.

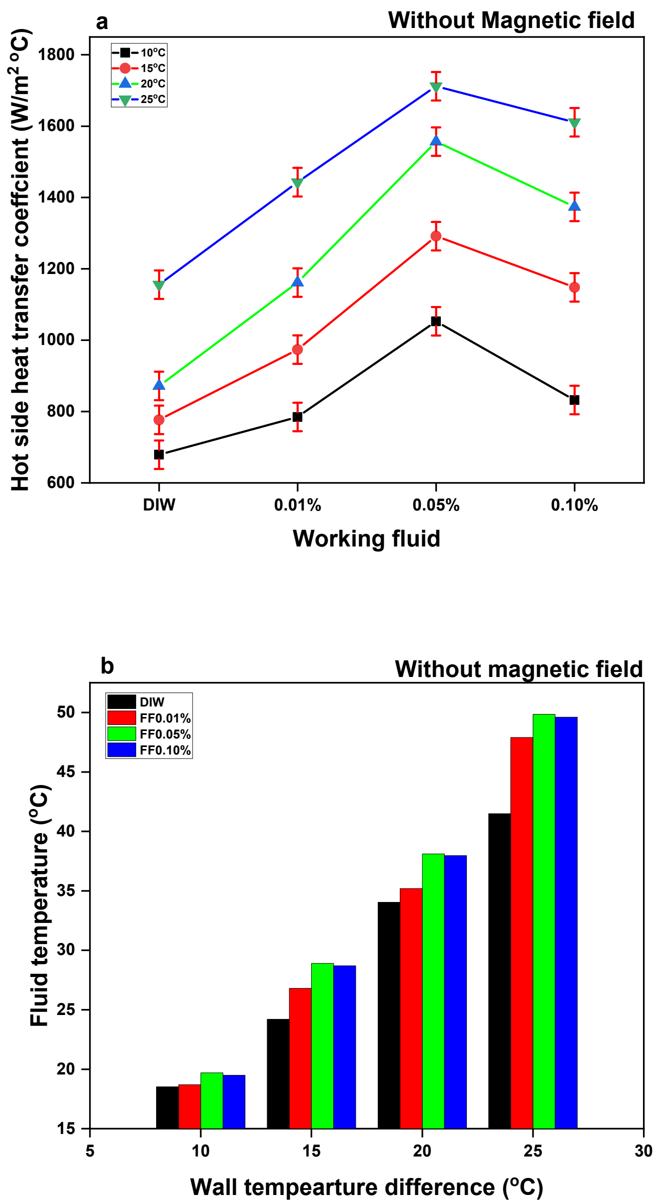

Fig. 7 Effect of volume fraction on a) hot side heat transfer coefficient of the cavity without Magnetic field at different ΔT_{hc}; and b) working fluid temperature inside the cavity

Table 4 represents the improvement in thermophysical properties of $MgFe_2O_4$ FF at different volume fractions compared to that of water at a temperature 25 ºC. It is noted that the thermal conductivity of FF is enhanced greater at volume fraction 0.05% compared to the FF volume fraction of 0.01% and base fluid. At the same time, there is no significant enhancement in thermal conductivity of FF for 0.10% compared to the 0.05% volume fraction of $MgFe_2O_4$. On the other hand, the viscosity and density of 0.10% volume fraction are higher than that of volume fraction 0.05% and 0.01%. As a result, the ratio of coefficient enhancement between viscosity and thermal conductivity is more at a volume fraction of 0.10% and it indicates that the effect of viscosity is dominant than the effect of thermal conductivity at the volume fraction of 0.1%. Therefore, the heat transfer from the hot sidewall to FF at volume fraction 0.10% is lower than the same of 0.05%, consequently, the temperature of FF at volume fraction 0.10% is lower than the same at 0.05% as shown in Figure 7(b). At volume fraction 0.10%, the agglomeration of the magnetic nanoparticle is high compared to lower volume fractions. As a response, the particle's Brownian motion within the fluid decreases, and the effect of thermal conductivity enhancement drops behind the influence of the fluid's increased viscosity and density. Figure 8(a) shows the enhancement in h_{hot} due to the influence of MF for 0.05% volume fraction of FF at different ΔT_{hc}. The increase in the MF from 0 to 350 Gauss improved the h_{hot} and it is enhanced by 15.95% compared to the same FF without MF application at $\Delta T_{hc} = 25$ ºC. The application of MF on the FF filled cubical cavity generates magnetic force through the FF and these magnetic forces in the fluid will raise the temperature of fluid leading to the enhancement of buoyant force inside the cavity. By applying the MF 350 Gauss, the temperature of the FF at 0.05% volume fraction improved over the same FF without MF as shown in Figure 8(b). This improvement in temperature is due to the effect of enhanced thermal conductivity of FF at 350 Gauss (around 10.72% improvement compared to base fluid), thus heat will transfer more from the hot sidewall to fluid. This reduces the density of the fluid and leads to the enhancement of buoyant force inside the cavity leading to the heat transfer enhancement.

Table 3 Percentage of enhancement in Thermo-physical properties of $MgFe_2O_4$ ferrofluid without magnetic field application

Volume fraction of $MgFe_2O_4$ ferrofluid	Thermal conductivity enhancement	Viscosity enhancement	Density enhancement	Ratio between coefficient of enhancement of viscosity and thermal conductivity
0.01%	1.84%	3.48%	0.64%	1.89
0.05%	6.87%	11.68%	1.72%	1.70
0.10%	7.53%	18.54%	3.10%	2.45

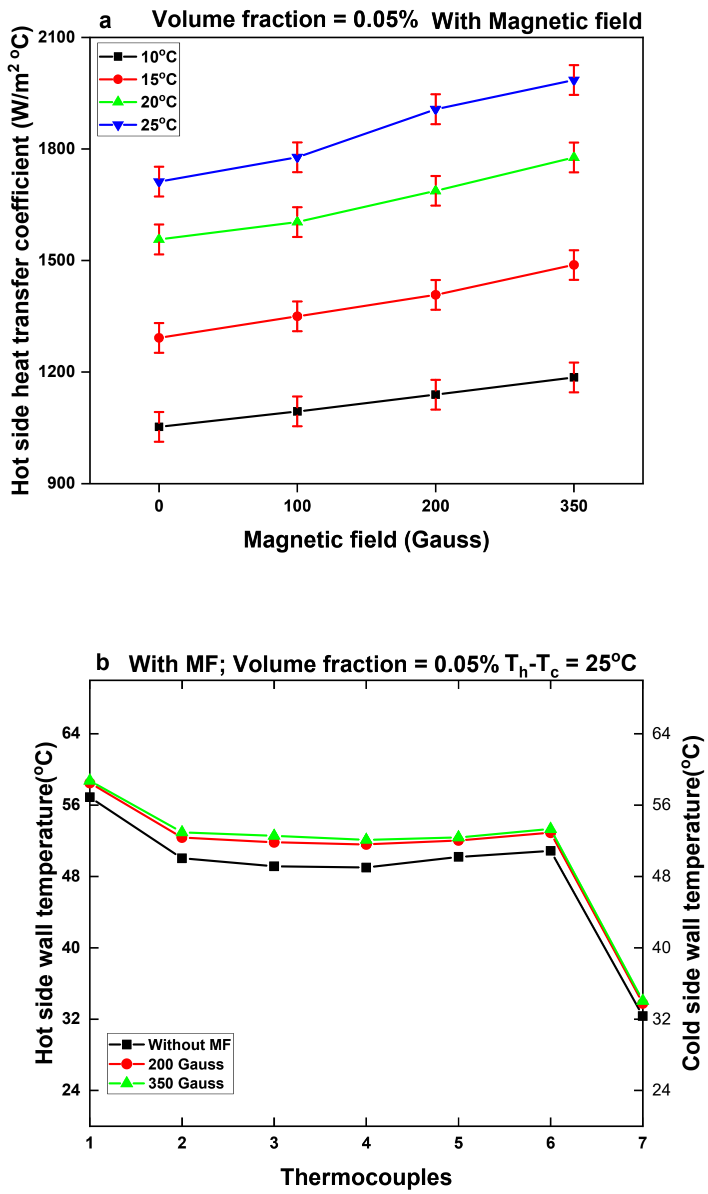

Fig. 8 Effect of magnetic field on a) hot side heat transfer coefficient of the cavity at different ΔT_{hc}; and b) the temperature variation inside the cavity at ΔT_{hc}=25°C for a volume fraction of 0.05%

Cold side heat transfer coefficient of the cavity

Though there is an enhancement in h_{hot} with the application of MF, a deterioration is noticed for the h_{cold} at the cold side. Figure 9(a) presents the h_{cold} for various volume fractions of FF with different ΔT_{hc} and indicates that the h_{cold} is lower than the cavity with deionized water due to its comparatively low viscosity and density at lower temperatures. The maximum percentage of deterioration of 9.59% occurred at a volume fraction of 0.10% in comparison with that of water. The h_{cold} of the cavity filled with water shows 355.984 W/m^2 C at ΔT_{hc} = 10 ºC. By increasing the ΔT_{hc} from 10 to 25 ºC, it enhanced to 730.034 W/m^2 ºC due to the improved buoyancy effect. By using the $MgFe_2O_4$ FF inside the cavity the h_{cold} of cavity reduced to 338.095 W/m^2 C, 324.583 W/m^2 ºC, and 321.339 W/m^2 ºC for volume fractions 0.01%, 0.05%, and 0.10% respectively at ΔT_{hc} = 10 ºC. At this ΔT_{hc}, the cold sidewall of the cavity is kept at a lower temperature (12 ºC). Owing to this lower temperature at the cold sidewall compared to the hot side wall (55 ºC), the FF near the cold sidewall experience higher density and viscosity, which results in the decrease of the buoyancy effect near the cold sidewall, which results in low heat transfer from the FF to the cold sidewall. It is also pointed out that the increase in ΔT_{hc} from 10 to 25 ºC enhances the h_{cold} cavity filled with $MgFe_2O_4$ FF due to the reduction in viscosity and density of the fluid near the cold sidewall. At ΔT_{hc} = 25 ºC, the h_{cold} improved to 646.84, 617.01, and 613.041 W/m^2 ºC for volume fractions 0.01%, 0.05%, and 0.10% respectively. The h_{cold} of the cavity filled with $MgFe_2O_4$ FF by the MF influence at different ΔT_{hc} and volume fraction 0.05% is presented in Figure 9(b). The application of the MF consistently reduced the h_{cold} of the cavity filled with $MgFe_2O_4$ FF at all ΔT_{hc}. At ΔT_{hc} = 10ºC and volume fraction 0.05% the h_{cold} is 324.583 W/m^2 ºC without the application of MF and it is reduced to 304.67 W/m^2 ºC at 350 Gauss MF. This reduction in h_{cold} may be due to the development of a thermal boundary layer near the cold sidewall in the presence of the MF. By increasing the ΔT_{hc} from 10 to 25 ºC at 350 Gauss MF, the h_{cold} is improved from 304.67 to 579.53 W/m^2 C.

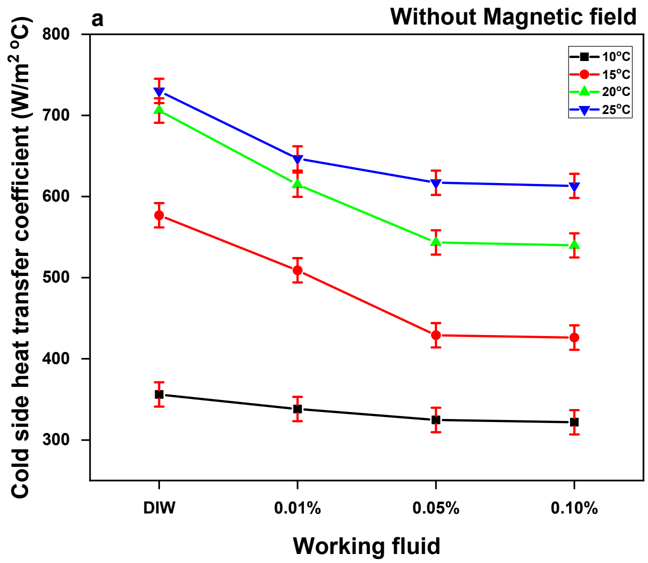

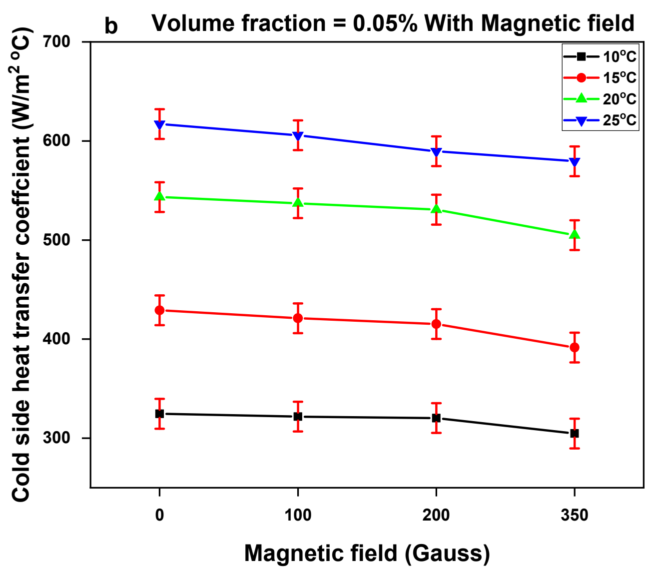

Fig. 9 Cold side heat transfer coefficient of the cavity a) at different volume fraction without Magnetic field ; and b) at a volume fraction 0.05% $MgFe_2O_4$ ferrofluid for different magnetic field and ΔT_{hc}

Average heat transfer coefficient of the cavity

The average heat transfer coefficient of cavity h_{avg} with FF is higher than the cavity with water since the effect of h_{hot} dominates over the h_{cold} of the cavity, as presented in Figure 10. The highest improvement of 23.51% is observed in FF filled cavity for a volume fraction of 0.05% compared to the water-filled cavity at ΔT_{hc} = 25 °C (enhanced from 942.88 to 1164.53 W/m^2 C). This enhancement in the h_{avg} at volume fraction 0.05% is higher than the results obtained by Giwa et al.(2020b, c) for Fe_2O_3:Al_2O_3/ water hybrid NF (11.92% for 0.10% volume fraction) and Fe_2O_3: MWCNT/water hybrid FF (11.59% enhancement for 0.05% volume fraction). Further, the surge in the MF from 0 to 350 Gauss enhanced the h_{avg} at all ΔT_{hc}. The highest improvement of 10.11% in the h_{avg} observed for the FF at a volume fraction of 0.05%, 350 Gauss, and 25°C compared to that of the same volume fraction of FF without MF application (enhanced from 1164.53 to 1282.362 W/m^2 °C).

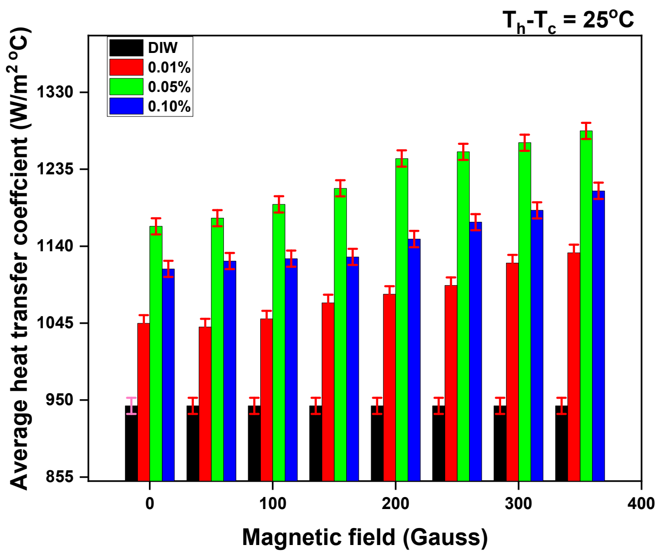

Fig. 10 Effect of magnetic field on average heat transfer coefficient of the cavity at different volume fractions (0.01%,0.05% and 0.10%) of $MgFe_2O_4$ ferrofluid and ΔT_{hc}=25°C

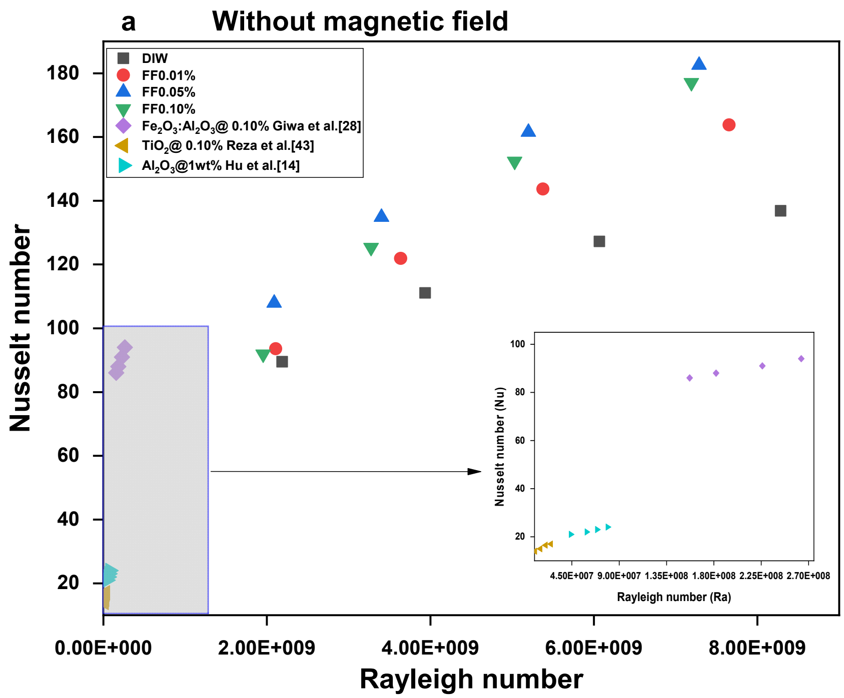

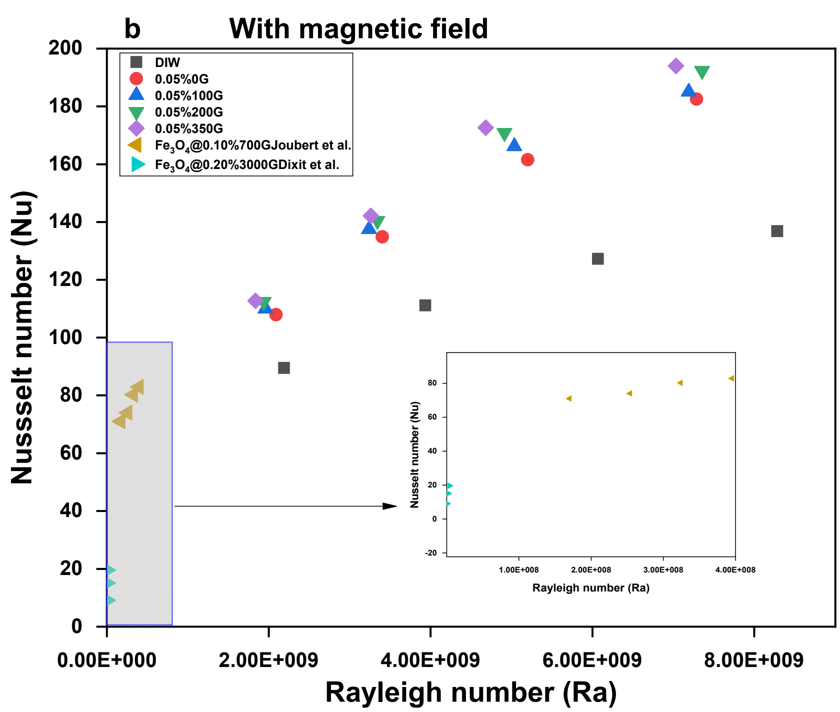

Fig. 11 Influence of Rayleigh number on Nusselt number a) at different volume fractions of $MgFe_2O_4$ ferrofluid in the absence of MF; b) with the application of magnetic field at volume fraction 0.05%

Relation for Nu and Ra of the cavity

Figure 11(a) describes the change in Nu_{avg} with respect to the variation in the Ra for FF-filled cavity in the absence of MF. The Ra for the water-filled cavity was in the range of 2.20×10^9 to 8.30×10^9 for the ΔT_{hc} in the range of 10 to 25 °C. Increasing the wall temperature often raises the Ra due to the reduction of viscous force and the rise of the buoyancy force leading to fluid motion in the cavity which in turn increases the Nu_{avg}. The dispersal of $MgFe_2O_4$ nanoparticles in the water was noted as the cause for lowering of the Ra at all ΔT_{hc} in relation to base fluid with a comparative rise in the Nu_{avg} at all volume fractions. This analysis shows that the Nu_{avg} inside the cavity is improving with the rise in ΔT_{hc} and it indicates that temperature rise improves the buoyancy force of working fluid inside the cavity. The cavity filled with $MgFe_2O_4$ FF at volume fraction 0.05% exhibited a higher Nu_{avg} of 182.5 at $Ra = 7.29\times 10^9$ and $\Delta T_{hc} = 25$°C compared to that of base fluid (enhanced by 33.37%). The observed Nu_{avg} at this temperature is comparatively higher than the obtained values of Brusly Solomon et al. (2017a) for Al_2O_3/EG NF at 0.05% volume fraction and Joubert et al.(2017) for Fe_3O_4/Water FF. Nu_{avg} obtained for various NFs filled in the rectangular cavity (Reza et al. 2011; Hu et al. 2014; Giwa et al. 2020b) is compared with the present study and it showed a huge enhancement in Nu_{avg} owing to the enhancement in buoyancy in the cavity due to its lower viscosity and density.

The influence of the MF application on the FF-filled cubical cavity charged at this optimum volume fraction is represented in Figure 11(b). By the influence of MF from 0 to 350 Gauss, the Nu_{avg} of the FF charged cavity at volume fraction 0.05% is enhanced from 182.5 to 194.003 (6.28% enhancement) at 25 °C. This results in the augmentation of the Nu_{avg} in the presence of MF and is comparable with the results obtained by Giwa et al. (2020c) for 0.05% volume fraction of Fe_2O_3: MWCNT/water hybrid FF in the presence of MF strength 219.5 Gauss (5.02% enhancement). And slightly higher than the results obtained by Joubert et al.(2017) for 0.10% volume fraction of Fe_2O_3/water FF in the presence of MF strength 700 Gauss (2.81% enhancement). The Nu_{avg} reported for Fe_3O_4 FF by Joubert et al.(2017) and Dixit and Pattamatta (2020) at higher MF 700 Gauss and 3000 Gauss are lower than that of the present study as shown in Figure 11(b). Table 5 presents the improvement in NC heat transfer in different cavities used by different NF. From this analysis, it can be concluded that $MgFe_2O_4$ FF exhibits more improvement in heat transfer compared to that of other NF except for MWCNT: Water NF.

Table 4 Natural convection heat transfer improvement in different cavity with various NF

Authors	Type of nanofluid	Geometry of cavity	Heat transfer enhancement
Brusly Solomon et al. (2017a)	Al_2O_3 + Ethylene glycol	Square	10% enhancement at volume fraction 0.05%
Sharifpur et al.(2018)	TiO_2 + Water	Square	8.2% enhancement at volume fraction 0.05%
Garbadeen et al.(2017)	MWCNT + Water	Square	45% enhancement at volume fraction 0.10%
Ghodsinezhad et al.(2016)	Al_2O_3 + Water	Rectangular	15% enhancement at volume fraction 0.10%
Giwa et al.(2019)	Al_2O_3:MWCNT(60:40 wt%) + Water	Square	20.5% enhancement at volume fraction 0.10%
Hu et al.(2014)	Al_2O_3 + Water	Square	7% enhancement at 1wt%
Ilyas et al.(2017)	Al_2O_3 + Thermal oil	Rectangular	2.72% enhancement at 0.5wt%
Joubert et al.(2017)	Fe2O3 + Water	Square	5.63% enhancement at volume fraction 0.10%. Further enhancement of 2.81% at 700 Gauss MF
Lei et al.(2019)	Fe_3O_4:CNT + Water	Rectangular	15% enhancement in at 2:1 mass fraction. Further enhanced from 15% to 24% with the application of MF 400 Gauss
Giwa et al.(2020b)	Fe_2O_3:Al_2O_3 + Water	Rectangular	10.81% enhancement at volume fraction 0.10%. Further improved by 4.91% at MF 219.5 Gauss
Giwa et al.(2020c)	Fe_2O_3:MWCNT + Water	Rectangular	11.21% enhancement at volume fraction 0.05%. Again, enhanced by 5.02% at MF 219.5 Gauss
Present Study	$MgFe_2O_4$ + Water	Cubical cavity	33.37% enhancement at volume fraction 0.05%. Again, enhanced by 6.28% at MF 350 Gauss

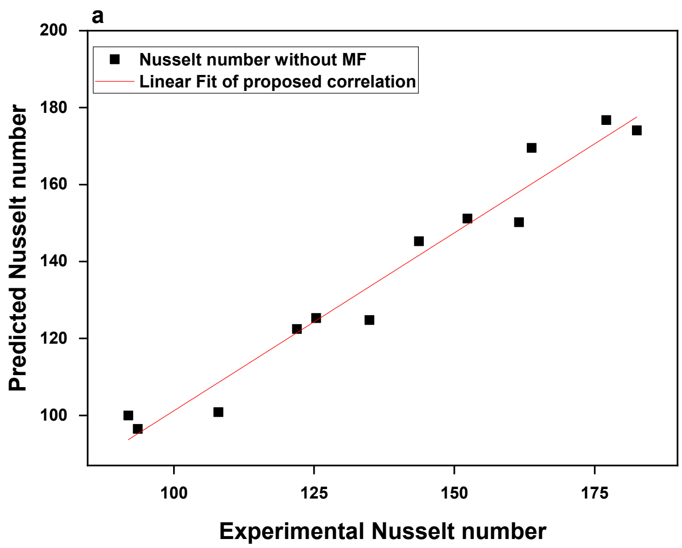

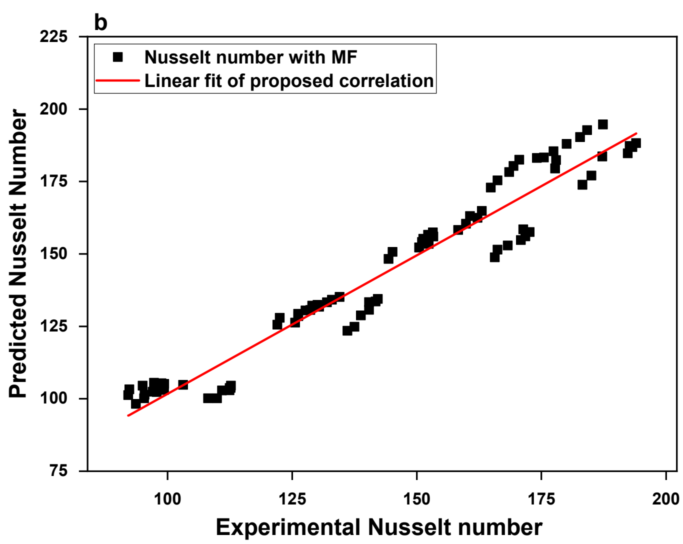

Fig. 12 Validation of experimental and predicted Nusselt number a) in the absence of Magnetic field; b) in the presence of Magnetic field

Proposed correlation for Nusselt number

To predict the Nu_{avg} inside the FF-filled cubical cavity in the nonattendance and attendance of MF, new correlations are derived as functions of volume fraction of FF, *Ra*, and applied MF as shown in Eqs. (15) and (16). Figures 12(a) and (b) present the validation of the predicted Nu_{avg} with the experimental Nu_{avg} without and with MF influence.

$$\mathrm{Nu} = 0.009247[1+\phi]^{0.02984}[\mathrm{Ra}]^{0.4373} \quad ; R^2 = 0.92 \qquad (15)$$

This proposed correlation may accurately predict the experimental Nusselt number with a margin of error -8.81 % and 7.48% with mean absolute deviation of 0.82 %.

$$\mathrm{Nu} = 0.007822[1+\phi]^{0.74769}[\mathrm{Ra}]^{0.438429}\left[1+\frac{\mathrm{M}}{\mathrm{M_{max}}}\right]^{0.160954} \; ; R^2 = 0.94 \quad (16)$$

The margin of deviation between experimental and predicted Nusselt number lies between -10.53% and 11.30% with mean absolute deviation of 0.17%.

Conclusion

Natural convection heat transfer performance of disk-shaped $MgFe_2O_4$ ferrofluid charged cubical cavity at different volume fractions was experimentally analyzed in the attendance of magnetic field ranging from 0 to 350 Gauss. The buoyancy effect in the cavity was developed by maintaining different wall temperature differences between the two vertical sidewalls of the cavity. From the results, significant improvements in h_{avg} and Nu_{avg} were observed for all volume fractions of $MgFe_2O_4$ ferrofluid in comparison with base fluid without the application of magnetic field on the ferrofluid charged cavity. The 0.05% volume fraction of $MgFe_2O_4$ ferrofluid shows the finest heat transfer performance with an enhancement of 23.51% to the h_{avg} and 33.37% to the Nu_{avg} when compared to the base fluid at ΔT_{hc} = 25ºC. By applying the magnetic field in the range of 0 to 350 Gauss, the heat transfer properties of ferrofluid were enhanced. By inducing 350 Gauss MF on ferrofluid charged cavity, the h_{avg} was enhanced from 23.51% to 36.003% and Nu_{avg} enhanced from 33.38% to 41.76% at volume fraction 0.05% and ΔT_{hc} = 25 ºC. Based on the previous experimental studies related to the natural convection using various types of ferrofluid, the present study concludes that the use of disk-shaped $MgFe_2O_4$ ferrofluid exhibits more heat transfer performance than other ferrofluids.

Acknowledgement

The authors are grateful to Mr. R. Jeyaseelan, Lab technician, Advanced thermal Sciences lab, Karunya Institute of Technology and Sciences, India, for his technical support.

References

Ahmed A, Baig H, Sundaram S, Mallick TK (2019) Use of Nanofluids in Solar PV / Thermal Systems. International Journal of Photoenergy 2019:. https://doi.org/10.1155/2019/8039129

Ajith K, Enoch IVM, Solomon AB, Sumohan A (2019) Characterization of magnesium ferrite nanofluids for heat transfer applications. Materials Today: Proceedings. https://doi.org/10.1016/j.matpr.2019.09.014

Ajith K, Pillai AS, Enoch IVMV, Solomon AB (2020) Effect of magnetic field on the thermophysical properties of low-density ferrofluid with disk-shaped MgFe2O4 nanoparticles. Colloids and Surfaces A: Physicochemical and Engineering Aspects 126083. https://doi.org/10.1016/j.colsurfa.2020.126083

Ajith K, Pillai AS, Muthu Vijayan Enoch IV, et al (2021) Effect of the non-electrically conductive spindle on the viscosity measurements of nanofluids subjected to the magnetic field. Colloids and Surfaces A: Physicochemical and Engineering Aspects 628:127252. https://doi.org/10.1016/j.colsurfa.2021.127252

Akilu S, Tesfamichael A, Sharma K V (2017) Experimental measurements of thermal conductivity and viscosity of ethylene glycol-based hybrid nano fluid with TiO 2 -CuO / C inclusions. Journal of Molecular Liquids 246:396–405. https://doi.org/10.1016/j.molliq.2017.09.017

B. Berkovsky VP Numerical study of problems on high-intensive free convection. in: Proc Int Turbul Buoyant Convect Semin, 148:148–162

Brusly Solomon A, Sharifpur M, Ottermann T, et al (2017) Natural convection enhancement in a porous cavity with Al2O3-Ethylene glycol/water nanofluids. International Journal of Heat and Mass Transfer 108:1324–1334. https://doi.org/10.1016/j.ijheatmasstransfer.2017.01.009

Choi SUS (1995) Enhancing thermal conductivity of fluids with nanoparticles. American Society of Mechanical Engineers, Fluids Engineering Division (Publication) FED 231:99–105

Choudhary R, Subudhi S (2016) Aspect ratio dependence of turbulent natural convection in Al 2 O 3 / water nanofluids. Applied Thermal Engineering 108:1095–1104. https://doi.org/10.1016/j.applthermaleng.2016.08.016

Dixit DD, Pattamatta A (2019) Natural convection heat transfer in a cavity filled with electrically conducting nano- particle suspension in the presence of magnetic field. Physics of Fluids 023302: https://doi.org/10.1063/1.5080778

Dixit DD, Pattamatta A (2020) Effect of uniform external magnetic-field on natural convection heat transfer in a cubical cavity filled with magnetic nano-dispersion. International Journal of Heat and Mass Transfer 146:118828. https://doi.org/10.1016/j.ijheatmasstransfer.2019.118828

Doganay S, Alsangur R, Turgut A (2019) Effect of external magnetic field on thermal conductivity and viscosity of magnetic nanofluids: A review. Materials Research Express 6:. https://doi.org/10.1088/2053-1591/ab44e9

Ebrahimi A, Tamnanloo J, Mousavi SH, et al (2021) Discrete-Continuous Genetic Algorithm for Designing a Mixed Refrigerant Cryogenic Process. Industrial and Engineering Chemistry Research 60:7700–7713. https://doi.org/10.1021/acs.iecr.1c01191

Elsheikh AH, Sharshir SW, Mostafa ME, et al (2018) Applications of nanofluids in solar energy: A review of recent advances. Renewable and Sustainable Energy Reviews 82:3483–3502. https://doi.org/10.1016/j.rser.2017.10.108

Gaganpreet, Srivastava S (2012) Effect of aggregation on thermal conductivity and viscosity of nanofluids. Applied Nanoscience 2:325–331. https://doi.org/10.1007/s13204-012-0082-z

Garbadeen ID, Sharifpur M, Slabber JM, Meyer JP (2017) Experimental study on natural convection of MWCNT-water nano fl uids in a square enclosure. International Communications in Heat and Mass Transfer 88:1–8. https://doi.org/10.1016/j.icheatmasstransfer.2017.07.019

Ghasemi H, Darjani S, Mazloomi H, Mozaffari S (2020) Preparation of stable multiple emulsions using food-grade emulsifiers: evaluating the effects of emulsifier concentration, W/O phase ratio, and emulsification process. SN Applied Sciences 2:1–9. https://doi.org/10.1007/s42452-020-03879-5

Ghasemi H, Mozaffari S, Mousavi SH, et al (2021) Decolorization of wastewater by heterogeneous Fenton reaction using MnO2-Fe3O4/CuO hybrid catalysts. Journal of Environmental Chemical Engineering 9:105091. https://doi.org/10.1016/j.jece.2021.105091

Ghodsinezhad H, Sharifpur M, Meyer JP (2016) Experimental investigation on cavity flow natural convection of Al2O3–water nanofluids. International Communications in Heat and Mass Transfer 76:316–324. https://doi.org/10.1016/j.icheatmasstransfer.2016.06.005

Giwa SO, Sharifpur M, Ahmadi MH, Meyer JP (2021) A review of magnetic field influence on natural convection heat transfer performance of nanofluids in square cavities. Springer International Publishing

Giwa SO, Sharifpur M, Ahmadi MH, Meyer JP (2020a) Magnetohydrodynamic convection behaviours of nanofluids in non-square enclosures: A comprehensive review. Mathematical Methods in the Applied Sciences. https://doi.org/10.1002/mma.6424

Giwa SO, Sharifpur M, Meyer JP (2019) Experimental study of thermo-convection performance of hybrid nanofluids of Al 2 O 3 -MWCNT / water in a differentially heated square cavity. International Journal of Heat and Mass Transfer 119072. https://doi.org/10.1016/j.ijheatmasstransfer.2019.119072

Giwa SO, Sharifpur M, Meyer JP (2020b) E ff ects of uniform magnetic induction on heat transfer performance of aqueous hybrid ferro fluid in a rectangular cavity. 170:. https://doi.org/10.1016/j.applthermaleng.2020.115004

Giwa SO, Sharifpur M, Meyer JP (2020c) Experimental investigation into heat transfer performance of water-based magnetic hybrid nanofluids in a rectangular cavity exposed to magnetic excitation. International Communications in Heat and Mass Transfer 116:104698. https://doi.org/10.1016/j.icheatmasstransfer.2020.104698

Hu Y, He Y, Qi C, et al (2014) Experimental and numerical study of natural convection in a square enclosure filled with nanofluid. International Journal of Heat and Mass Transfer 78:380–392. https://doi.org/10.1016/j.ijheatmasstransfer.2014.07.001

Joubert JC, Sharifpur M, Solomon AB, Meyer JP (2017) Enhancement in heat transfer of a ferrofluid in a differentially heated square cavity through the use of permanent magnets. Journal of Magnetism and Magnetic Materials 443:149–158. https://doi.org/10.1016/j.jmmm.2017.07.062

Kumar A, Subudhi S (2017) Preparation, characteristics, convection and applications of magnetic nanofluids: A review. https://doi.org/10.1007/s00231-017-2114-4

Mojumder S, Saha S, Saha S, Mamun MAH (2015) Effect of magnetic field on natural convection in a C -shaped cavity filled with ferrofluid. Procedia Engineering 105:96–104. https://doi.org/10.1016/j.proeng.2015.05.012

Mozaffari S, Ghasemi H, Tchoukov P, et al (2021) Lab-on-a-Chip Systems in Asphaltene Characterization: A Review of Recent Advances. Energy and Fuels 35:9080–9101. https://doi.org/10.1021/acs.energyfuels.1c00717

Narankhishig Z, Ham J, Lee H, Cho H (2021) Convective heat transfer characteristics of nanofluids including the magnetic effect on heat transfer enhancement - a review. Applied Thermal Engineering 193:116987. https://doi.org/10.1016/j.applthermaleng.2021.116987

Nkurikiyimfura I, Wang Y, Pan Z (2013) Heat transfer enhancement by magnetic nanofluids — A review. Renewable and Sustainable Energy Reviews 21:548–561. https://doi.org/10.1016/j.rser.2012.12.039

Reza M, Mahrood K, Etemad SG, Bagheri R (2011) Free convection heat transfer of non Newtonian nano fluids under constant heat flux condition ☆. International Communications in Heat and Mass Transfer 38:1449–1454. https://doi.org/10.1016/j.icheatmasstransfer.2011.08.012

Sathyamurthy R, Kabeel AE, Chamkha A, et al (2021) Experimental investigation on cooling the photovoltaic panel using hybrid nanofluids. Applied Nanoscience (Switzerland) 11:363–374. https://doi.org/10.1007/s13204-020-01598-2

Sezer N, Atieh MA, Koç M (2019) A comprehensive review on synthesis, stability, thermophysical properties, and characterization of nanofluids. Powder Technology 344:404–431. https://doi.org/10.1016/j.powtec.2018.12.016

Sha L, Ju Y, Zhang H, Wang J (2017) Experimental investigation on the convective heat transfer of Fe 3 O 4 / water nanofluids under constant magnetic field. Applied Thermal Engineering 113:566–574. https://doi.org/10.1016/j.applthermaleng.2016.11.060

Shah J, Ranjan M, Davariya V, et al (2017) Temperature-dependent thermal conductivity and viscosity of synthesized a-alumina nanofluids. Applied Nanoscience (Switzerland) 7:803–813. https://doi.org/10.1007/s13204-017-0594-7

Sheikholeslami M, Rokni HB (2017) Simulation of nanofluid heat transfer in presence of magnetic field: A review. International Journal of Heat and Mass Transfer 115:1203–1233. https://doi.org/10.1016/j.ijheatmasstransfer.2017.08.108

Shi L, He Y, Hu Y, Wang X (2019) Controllable natural convection in a rectangular enclosure filled with Fe 3 O 4 @ CNT nanofluids. International Journal of Heat and Mass Transfer 140:399–409. https://doi.org/10.1016/j.ijheatmasstransfer.2019.05.104

Solangi KH, Kazi SN, Luhur MR, et al (2015) A comprehensive review of thermo-physical properties and convective heat transfer to nano fluids. Energy. https://doi.org/10.1016/j.energy.2015.06.105

Solomon AB, Rooyen J Van, Rencken M, et al (2017) Experimental study on the influence of the aspect ratio of square cavity on natural convection heat transfer with Al 2 O 3 / Water nano fluids. International Communications in Heat and Mass Transfer 88:254–261. https://doi.org/10.1016/j.icheatmasstransfer.2017.09.007

Soltani O, Akbari M (2016) Effects of temperature and particles concentration on the dynamic viscosity of MgO-MWCNT / ethylene glycol hybrid nano fluid: Experimental study. Physica E: Low-dimensional Systems and Nanostructures 84:564–570. https://doi.org/10.1016/j.physe.2016.06.015

Vanaki SM, Ganesan P, Mohammed HA (2016) Numerical study of convective heat transfer of nano fluids: A review. Renewable and Sustainable Energy Reviews 54:1212–1239. https://doi.org/10.1016/j.rser.2015.10.042

Wang X, Zhang R, Mozaffari A, et al (2021) Active motion of multiphase oil droplets: emergent dynamics of squirmers with evolving internal structure. Soft Matter 17:2985–2993. https://doi.org/10.1039/d0sm01873b

Yu W, Xie H, Chen L, Li Y (2010) Enhancement of thermal conductivity of kerosene-based Fe3O4 nanofluids prepared via phase-transfer method. 355:109–113. https://doi.org/10.1016/j.colsurfa.2009.11.044

Nomenclature

$MgFe_2O_4$	Magnesium Ferrite
NF	Nanofluid
FF	Ferrofluid
MF	Magnetic Field
H_2O	Water
SDS	Sodium Dodecyl Sulfate
T	Temperature, °C
Q	Heat transfer, W
V	Voltage, v
I	Current, A
m	Mass flow rate, kg/ second
C_p	Specific heat, J/kg °C
h	heat transfer coefficient, W/ m^2 °C
A	Area of the cavity, m^2
Nu	Nusselt number
L_c	characteristic length of cavity, m
Ra	Rayleigh number
Pr	Prandtl number
L	Length, m
W	Width, m
H	Height, m
g	Acceleration due to gravity, m^2/s
Greek Symbols	
k	thermal conductivity, W/m °C
μ	dynamic viscosity (Cp)
ρ	density (kg/m^3)
β	thermal expansion coefficient, 1/K
Φ	volume fraction (%)
Δ	difference
∂	partial derivative
Subscripts	
nf	nanofluid
bf	base fluid
wf	working fluid
w	water
np	nanoparticles
in	input
out	output
avg	Average
hot	hot side
cold	cold side
hc	hot and cold side

STATEMENTS AND DECLARATION

Conflict of Interest

We wish to confirm that the present manuscript titled "***Turbulent magnetohydrodynamic natural convection in a heat pipe assisted cavity using disk-shaped magnesium ferrite nanoparticles***" authored by *K. Ajith, Mallolu Jesse Aaron, Archana Sumohan Pillai, I. V. Muthu Vijayan Enoch, M. Sharifpur, A. Brusly Solomon, and J.P. Meyer* is a new research work carried out at our institution. We wish to confirm that there is no conflict of interest among the co-authors. And the Authors declare that they have no known competing financial interests or personal relationships that could have appeared to influence the work reported in this paper.

CRediT Author Statement

We wish to confirm that the following are the contribution made by each author of this article titled "**Turbulent magnetohydrodynamic natural convection in a heat pipe assisted cavity using disk-shaped magnesium ferrite nanoparticles**" authored by *K. Ajith, Mallolu Jesse Aaron, Archana Sumohan Pillai, I. V. Muthu Vijayan Enoch, M. Sharifpur, A. Brusly Solomon, and J.P. Meyer*

K. Ajith	Investigation, Validation, Writing – Original Draft
Mallolu Jesse Aaron	Investigation, Methodology
Archana Sumohan Pillai	Investigation, Methodology
I. V. Muthu Vijayan Enoch	Methodology, Reviewing, and Editing
M. Sharifpur	Reviewing and Editing
A. Brusly Solomon	Conceptualization, Supervision, Project administration, Reviewing and Editing
J.P. Meyer	Project administration

We confirm that this manuscript is not published before nor submitted to any other journal to consider publication.

Yours truly

Dr. A. Brusly Solomon, M.E., Ph.D.,
Associate Professor,
Department of Mechanical Engineering,
Karunya Institute of Technology and Sciences.
Coimbatore – 641 114
Tel: 0422-2614059
Mobile: 8220023860
Email: abruslysolomon@gmail.com
Mohsen.Sharifpur@up.ac.za